JOURNAL OF VIROLOGY, Dec. 2009, p. 12590–12600 Vol. 83, No. 23
0022-538X/09/$12.00 doi:10.1128/JVI.02643-08

Hepatitis C Virus Causes Uncoupling of Mitotic Checkpoint and Chromosomal Polyploidy through the Rb Pathway▽†

Keigo Machida,[1] Jian-Chang Liu,[1] George McNamara,[2] Alexandra Levine,[3] Lewei Duan,[1] and Michael M. C. Lai[1,4]*

Department of Molecular Microbiology and Immunology, University of Southern California, Keck School of Medicine, Los Angeles, California 90033[1]; Saban Research Institute, Los Angeles Children's Hospital, Los Angeles, California[2]; City of Hope, Duarte, California[3]; and Institute of Molecular Biology, Academia Sinica, Taipei 115, Taiwan[4]

Received 23 December 2008/Accepted 8 September 2009

Hepatitis C virus (HCV) infection is associated with the development of hepatocellular carcinoma and probably also non-Hodgkin's B-cell lymphoma. The molecular mechanisms of HCV-associated carcinogenesis are unknown. Here we demonstrated that peripheral blood mononuclear cells obtained from hepatitis C patients and hepatocytes infected with HCV in vitro showed frequent chromosomal polyploidy. HCV infection or the expression of viral core protein alone in hepatocyte culture or transgenic mice inhibited mitotic spindle checkpoint function because of reduced Rb transcription and enhanced E2F-1 and Mad2 expression. The silencing of E2F-1 by RNA interference technology restored the function of mitotic checkpoint in core-expressing cells. Taken together, these data suggest that HCV infection may inhibit the mitotic checkpoint to induce polyploidy, which likely contributes to neoplastic transformation.

Hepatitis C virus (HCV) infection is a potent risk factor for the development of hepatocellular carcinoma (59) and probably also non-Hodgkin's B-cell lymphoma (10), although the latter case is still controversial. Chromosomal abnormalities are common in hepatitis C patients and may reflect disease severity in the progression to cancer (21). Physical or chemical agents or oncogenic viruses commonly induce karyotypic abnormalities in cells (3). Genomic instability, one of the hallmarks of malignant transformation, promotes chromosomal translocations, gene amplifications, polyploidy, and chromosome deletions, resulting in loss of heterozygosity (25). Loss-of-heterozygosity events, involving the activation of proto-oncogenes or the inactivation of tumor suppressors, may provoke unrestrained cell growth and lead to malignant transformation (63). Previously, we have demonstrated that HCV infection induces a mutator phenotype by enhancing DNA double-strand breaks, leading to hypermutation of immunoglobulin, proto-oncogenes, and tumor suppressor genes (30).

This finding suggests that genomic alterations induced by viral genes may be one of the mechanisms of HCV oncogenesis. However, the molecular mechanism of chromosomal alterations associated with HCV infection has not been elucidated.

HCV contains an RNA genome that encodes 10 viral proteins. Among all of the HCV proteins, the core protein has been shown to have oncogenic potential. The expression of core protein can transform certain cell lines (42), and core protein-expressing transgenic mice develop tumors at an increased frequency (36). Furthermore, core protein has been shown to impair cell cycle regulation in stably transformed Chinese hamster ovary cells (16). Core protein also affects the function of human Rb, LZIP (a homologue to the *Drosophila melanogaster* BBF2/dCREB-A protein), and other cell growth regulatory proteins, such as 14-3-3 (1, 4, 13, 20, 61). The Rb gene can uncouple cell cycle progression from mitotic control by activation of mitotic checkpoint protein Mad2, leading to genomic instability (14).

Karyotype analysis is routinely performed in peripheral blood mononuclear cells (PBMCs). A hepatocyte in vitro culture system that mimics HCV infection of cells in hepatitis C patients was previously developed (64). We utilized this system to characterize the possible effects of HCV infection on chromosome stability. We showed that HCV infection in vitro induced multiple chromosomal abnormalities, including polyploidy. These effects can be mimicked by the expression of the HCV core protein alone. Based on the observation that the Rb defects promote genomic instability by uncoupling cell cycle progression from mitotic control, leading to genomic instability (14), we hypothesized and demonstrated that inhibition of Rb expression is the key event for chromosomal instability in HCV-infected cells. We further demonstrated that downregulation of Rb expression by HCV infection or core protein alone leads to sequential E2F-1 and Mad2 overexpression, which results in uncoupling of mitotic checkpoint. This study provides insights into novel mechanisms of oncogenesis for an RNA virus, which does not possess the classical oncogenes and does not integrate into chromosome.

MATERIALS AND METHODS

PBMCs. Eight HCV$^+$ PBMCs, six HCV$^-$ PBMCs from hepatitis C patients, and seven PBMCs from healthy individuals were analyzed. Aneuploidy or polyploidy was scored separately from translocations, gaps, and fragments, since they most likely result from very different mechanisms. The HCV infection status of patients and healthy controls was verified by reverse transcription-PCR (RT-PCR) detection of intracellular viral RNA. The demographic information of both groups was comparable.

* Corresponding author. Mailing address: Department of Molecular Microbiology and Immunology, University of Southern California, Keck School of Medicine, Los Angeles, CA 90033. Phone: (323) 442-1748. Fax: (323) 442-1721. E-mail: michlai@usc.edu.

† Supplemental material for this article may be found at http://jvi.asm.org/.

▽ Published ahead of print on 30 September 2009.

Cell culture. Hep-neo, Hep-core, 293-neo, and 239-core were generated by transfection in HepG2 or HEK293 cells and selection of clones. Linearized core protein expression vectors were transfected and treated with antibiotics to select for transfectants. Several colonies were isolated and confirmed for HCV core protein expression. Primary hepatocytes were obtained from Cell Culture Core Facility at the University of Southern California. Cultured or freshly isolated human hepatocytes were prepared according to published methods (45). Cells were cultured in Dulbecco's modified Eagle's medium (DMEM) supplemented with 10% fetal bovine serum (FBS), 0.2% bovine serum albumin, hydrocortisone (50 μM), and insulin (10 μg/ml) on dishes precoated with rat tail collagen and incubated at 37°C. Raji cells were obtained from ATCC. JT cells, an Epstein-Barr virus-transformed B-cell line, were established from a healthy individual as previously described (57). Raji cells and JT cells were grown in RPMI 1640 (Invitrogen, Carlsbad, CA) containing 20% FBS for Raji cells and 10% FBS for JT cells. Raji and JT cells were further cloned by single-cell dilution and then used for HCV infection using the culture supernatant of an HCV-producing B-cell line (SB cells) derived from an HCV^+ non-Hodgkin's lymphoma (57). A control infection using UV-irradiated SB cell culture supernatant was included in all of the experiments. The HCV-infected cells were split every 4 days. The JFH-1 strain was a gift from T. Wakita (National Institute of Infectious Diseases, Japan) and J. Liang (National Institutes of Health) (64). HepG2, Huh7, and Huh7.5.1 cells (a generous gift from F. V. Chisari at the Scripps Research Institute), HEK293 cells, and mouse embryo fibroblasts (MEFs) were cultured in DMEM containing 10% FBS. HEK293-core and Hep-core were generated by transfection of a linearized HCV core protein expression vector and selected with antibiotics for 2 weeks. 293-neo and Hep-neo were generated via similar methods using an empty linearized vector control plasmid. Cells were infected with high-titer recombinant retroviruses expressing E2F-1 (LPC-E2F-1) (38) or E2F-1 short hairpin RNA (shRNA) selected with puromycin (2 μg/ml) and nocodazole (Sigma) at 200 nM and 400 nM for the normal fibroblast and tumor cell lines, respectively.

Core protein-expressing transgenic mice. For the animal studies, transgenic mice expressing the HCV core protein of genotype 1b under the control of the human elongation factor 1a (EF-1a) promoter were generated and bred at the University of Southern California transgenic mouse facility (29). The primary MEFs were prepared from both the core protein-expressing transgenic mouse and its littermate embryos by trypsinizing the embryonic tissue and plating the dissociated cells. Splenocytes were obtained from spleen by standard procedures (53).

Karyotype analysis. Metaphase chromosomes were prepared by standard procedures (49). Cells were partially synchronized by colcemid (GibcoBRL; KaryoMAX colcemid solution) and sorted by staining with anti-core protein antibody, and chromosome spreads were prepared. For each experimental point, 50 to 100 metaphases were scored to determine the percentage of aberrant cells and the frequency of polyploidy. Chromosomal aberrations were defined using the nomenclature rules from the Committee on Standardized Genetic Nomenclature for Mice (see the Mouse Genome Informatics website at http://www.informatics.jax.org). Individual metaphase photographs were shuffled and scored blindly for the presence of structural chromosomal aberrations (48).

SKY. Multicolor spectral karyotyping (SKY) was done as previously described (27). In situ hybridization was performed by combining the SKY Paint-labeled DNA pools (Applied Spectral Imaging), using an SD-300/VDS-1300 spectral imager–charge-coupled device camera mounted on a Leica DMRXA fluorescence microscope, equipped with a Sutter LS-300 xenon arc lamp and a 1-m liquid light guide. Filter sets included the ASI SKY filter set for simultaneous imaging of Spectrum Green, Spectrum Orange, Texas Red, Cy5, and Cy5.5 fluorescent dyes and a Chroma 31000 DAPI (4′,6-diamidino-2-phenylindole) bandpass filter set. HCX PlanApo 40×/1.25 NA plus 1.6× Optovar or PL Apo 100×/1.4 NA oil immersion lenses (Leica) were used. SKY hybridization was performed according to the manufacturer's instructions, mounted with DAPI-VectaShield antifade solution (Vector Laboratories), and analyzed using the SkyVision 1.6.2 software. Seven to 40 metaphases were analyzed for each hepatocyte, splenocyte, or MEF preparation.

Perfusion and chromosome preparation. The livers of core protein-expressing transgenic and control mice were examined as previously described (46). Five animals per group were anesthetized, and the livers were perfused with a collagenase solution as described previously (32). After collagenase digestion, hepatocytes were separated by Percoll isodensity centrifugation and immediately plated in a 75-cm collagen type I-coated flask (Vitrogen 100; Celtrix Laboratories, Santa Barbara, CA) at a density of 5×10^6 cells (27) in 15 ml of 10% serum DMEM–F-12 medium, supplemented with 18 mM HEPES, 5 mM sodium pyruvate, 1 mM NaHCO, 1 mg/ml galactose, 30 μg/ml proline, 100 U/ml penicillin, 100/μg/ml streptomycin, and 1× ITS mixture (insulin, transferrin, and selenium; Invitrogen, Inc.). The medium was changed 2 h later, and 10 ng/ml murine epidermal growth factor (Invitrogen, Inc.) was added. Forty-four hours after plating, colcemid (Karyomax; Invitrogen, Inc.) was added to the medium. After an additional 2 to 3 h of incubation, the hepatocytes were removed from the dish with 0.25% trypsin solution and harvested for chromosome analysis by hypotonic treatment (0.075 M KCl) for 9.5 min (65). The hepatocytes were then further treated with 3:1 (vol/vol) acetic methanol fixative, and slides were prepared as described previously (47). Fifty G-banded metaphase spreads and SKY stainings of good morphology were randomly selected from cytogenetic preparations from each mouse.

Immunofluorescence. HCV-infected Raji cells were seeded onto sterile coverslips and irradiated from a ^{137}Cs source. At 6 h postirradiation, cells were fixed for 10 min in phosphate-buffered saline-buffered 3% paraformaldehyde–2% sucrose solution, followed by 5 min permeabilization on ice in Triton buffer (0.5% Triton X-100 in 20 mM HEPES, pH 7.4, 50 mM NaCl, 3 mM $MgCl_2$, 300 mM sucrose) for 5 min. These cells were immunostained with a monoclonal Mad2 antibody (Invitrogen), followed by a species-specific fluorochrome-conjugated secondary antibody (Jackson Immunoresearch) and photographed by confocal microscopy (Axiovert 35, Zeiss). For tubulin staining, antitubulin antibody (Sigma) and histone 2B (H2B)-green fluorescent protein (GFP) expression plasmids (pBOBH2BGFP; Clontech) were used.

Plasmids. The PCR-generated NS3, NS4B, NS5A, and NS5B cDNA fragment (genotype 1b and genotype H77) containing the Flag sequence was cloned into pcDNA3.1 (Invitrogen, Carlsbad, CA) as previously described (5, 62).

Mitotic spindle checkpoint assays. The ability of cells to complete mitosis was assayed by bromodeoxyuridine (BrdU) incorporation, since DNA synthesis occurs only after mitosis is completed (7). Log-phase cells were incubated with 0.27 μM colcemid for 24 h. During the final 4 h of incubation, 10 μM BrdU was added. Cells were fixed and analyzed for DNA content and incorporation of BrdU by flow cytometry as previously described (11). This analysis determines the defects of the mitotic checkpoint.

Transfection and reporter assay. Cells were transiently transfected using FuGENE transfection reagent (Boehringer Mannheim, Mannheim, Germany) with plasmids containing the luciferase reporter gene under the control of Rb, E2F-1 (Clontech), or the Mad2 promoter (17). Briefly, at 50% confluence, cells were transfected with a mixture of 1 μg of the reporter plasmid DNA and 3 μl of FuGENE reagent and incubated for 6 h at 37°C; then cells were washed and fresh medium was added. At 36 h posttransfection, the medium was replaced with fresh medium. Cells were harvested, and luciferase activity was determined using a Promega dual-luciferase reporter assay system. Cells were washed twice in phosphate-buffered saline and lysed by adding 200 μl of a lysis buffer (Promega). After 15 min at room temperature, the lysate was removed and centrifuged. To 20 μl of supernatant, 100 μl of a luciferase assay reagent was added, and firefly luciferase activity was measured in a Lumat LB9501 luminometer (Berthold, Wildbad, Germany) according to the manufacturer's guide. For the chloramphenicol acetyltransferase (CAT) assay, the Rb promoter CAT reporter plasmids were obtained from Wen-Hwa Lee of the University of California in Irvine. The FAST CAT assay kit (Molecular Probes) was used.

Statistical analysis. Statistical analysis of the data from aberrant chromosomes was performed by the χ^2 test. The t test was performed for a DNA damage sensitivity assay. P values of <0.05 were considered statistically significant.

RESULTS

HCV infection induces polyploidy. To determine whether HCV infection induces chromosomal aberrations, we performed karyotyping of the PBMCs from hepatitis C patients. Previously we have shown that PBMCs from some hepatitis C patients had enhanced mutations of multiple cellular genes (30). In this study, we further attempted to detect gross chromosomal aberrations and numerical changes of chromosomes by karyotyping analysis (SKY) (27, 49). HCV core protein and RNA in the PBMCs of the HCV^+ patients, but not healthy individuals, (Fig. 1A and B) were demonstrated by fluorescence-activated cell sorter (FACS) and seminested PCR, respectively. HCV RNA could be detected in PBMCs from 8 out of 14 hepatitis C patients (see Table S1 in the supplemental material). We found that PBMCs from HCV-infected patients showed chromosome polyploidy (Fig. 1C) significantly more

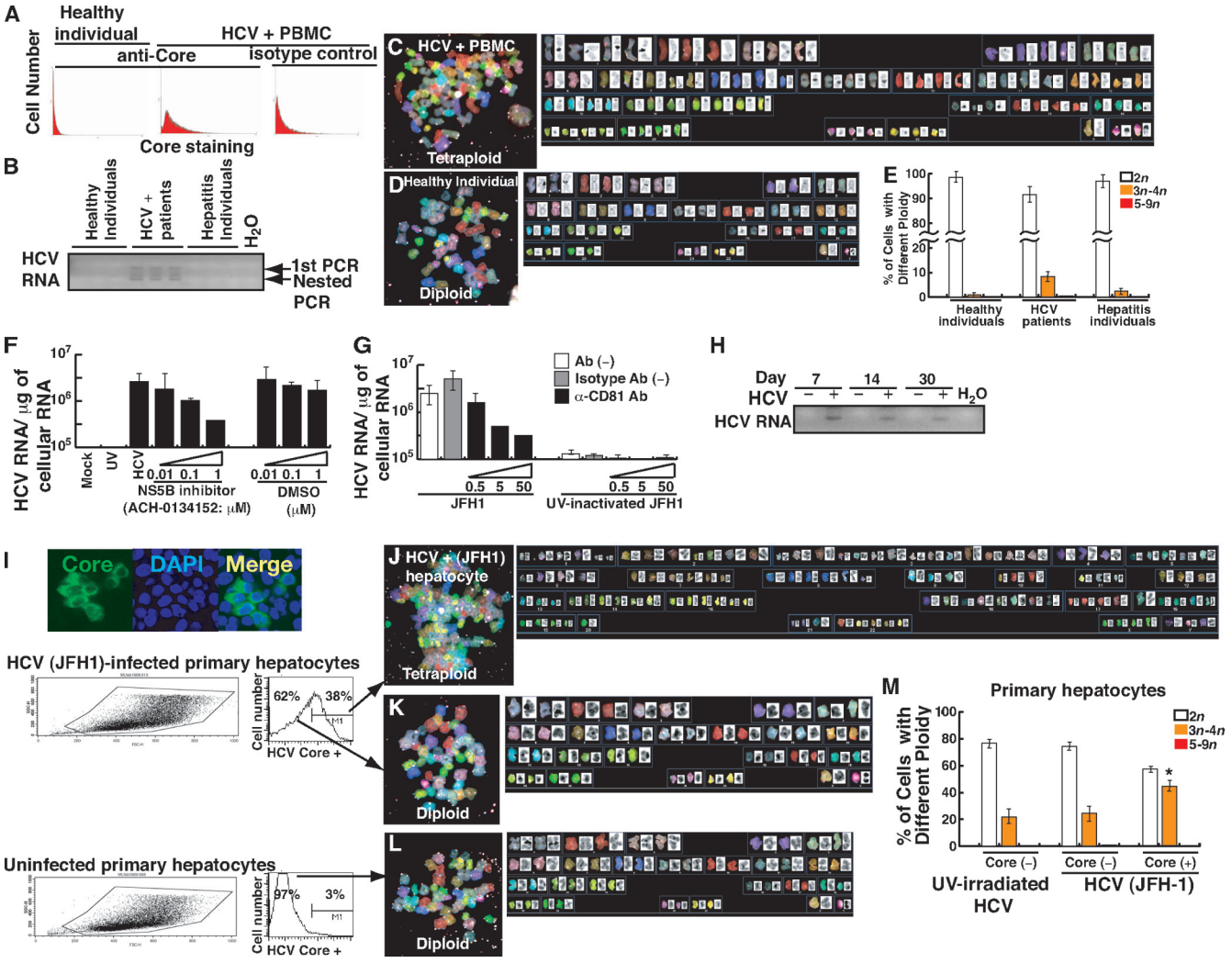

FIG. 1. Representative polyploidy in PBMCs of hepatitis C patients and HCV-infected culture cell lines. (A and B) Status of viral infection in PBMCs. HCV protein was detected by staining with anti-core protein antibody followed by FACS analysis (A), and HCV RNA was detected by RT-PCR analysis of HCV RNA (B). (C) Tetraploid metaphase from HCV-infected PBMCs. The figure includes the 4n chromosome number. (D) Diploid chromosome from a healthy individual. (E) Frequency of polyploidy in PBMCs from healthy individuals or HCV-infected patients and individuals with non-hepatitis C hepatitis. (F) HCV RNA levels in JFH-1-infected primary human hepatocytes treated with different concentrations of an NS5B inhibitor (ACS-0134152). HCV RNA levels were determined at 12 days postinfection. (G) Inhibition of HCV infection by anti-CD81 antibody. JFH-1 virus was preincubated with the indicated concentrations of anti-E2 antibody or irrelevant human immunoglobulin G1 isotype-matched antibody (Ab) for 1 h at 37°C before inoculation of primary hepatocytes. Total cellular RNA was analyzed by quantitative RT-PCR at day 8 postinfection. CD81-specific antibodies (α-CD81) reduced the amount of HCV RNA by about 70% compared to control antibody, confirming the specificity of the infection. (H) The status of HCV infection was verified by RT-PCR of HCV RNA at different time points after JFH-1 virus infection. (I) Immunostaining of core protein in HCV (JFH-1)-infected primary hepatocytes at day 12 postinfection. The infected cells were sorted by FACS using anti-core protein antibody. The infected and uninfected cells were used separately for karyotyping. (J, K, and L) Representative examples of tetraploid and diploid in HCV-infected or mock (UV-inactivated HCV)-treated primary hepatocytes. (M) Distribution of ploidy numbers in mock-infected and HCV-infected primary hepatocytes at 20 days postinfection.

frequently than PBMCs from healthy individuals (Fig. 1D and E; $P < 0.05$). Hepatitis patients from non-HCV sources did not show such a high frequency of polyploidy (Fig. 1E). Polyploidy most often occurred as tetraploid, but chromosome sets of a higher number have also been observed (Fig. 1E). In addition, translocations involving different pairs of chromosomes were frequently observed in these systems. Since polyploidy and translocation are caused by different mechanisms (33), we focused on polyploidy in this study.

To establish that the observed polyploidy phenotype was caused by HCV infection rather than as a result of inflammatory responses, we performed in vitro infection of human primary hepatocytes using a well-characterized hepatotropic strain of HCV, JFH-1 (64) (Fig. 1F to M). To establish that HCV RNA indeed replicated in the cells, the JFH-1-infected cells were pretreated with an NS5B inhibitor (ACH-0134152) and examined for HCV RNA by real-time RT-PCR at day 20 postinfection. The amounts of HCV RNA as detected by real-time RT-PCR were decreased by the NS5B inhibitor in a dose-dependent manner, indicating that the HCV RNA de-

tected indeed reflected HCV RNA replication in JFH-1-infected cells (Fig. 1F). Furthermore, to test the specificity of virus infection, we also examined the effects of neutralization with anti-CD81 antibody. The results showed that the level of HCV RNA was lowered by anti-CD81 in a dose-dependent manner, suggesting that the HCV RNA detected indeed represented specific infection of cells by HCV (Fig. 1G). Also, HCV-inoculated cells were treated with alpha interferon (IFN-α) and IFN-γ. The HCV RNA level was lowered by the IFN-α and -γ treatment in a dose-dependent manner (see Fig. S1 in the supplemental material). Finally, HCV RNA could be detected by RT-PCR for as long as 30 days after virus inoculation (Fig. 1H). Taken together, these results demonstrate that the HCV JFH-1 detected indeed represents real HCV RNA replication of human primary hepatocytes and not merely the attachment of the virus on the cell surface.

The infected primary hepatocytes expressing HCV core protein were sorted out (Fig. 1I), and the cells with and without the core protein were separately used for karyotype analysis (Fig. 1I to L). Uninfected and infected cells were examined at different time points after infection. Observers, blinded to the cells' identity, scored metaphase chromosome spreads prepared from the HCV-infected primary hepatocytes and uninfected counterparts. HCV-infected core protein-positive cells had a high frequency of cells exhibiting polyploidy (more than 46% at 10 days postinfection) (Fig. 1J). In contrast, only 21% of uninfected or mock-infected cells were polyploid (Fig. 1M). It is not clear why primary hepatocytes have a high background of chromosomal polyploidy; similar observations were made with mouse primary hepatocytes (see Fig. 3). Similar results were also obtained in lymphocytes infected with a lymphotropic strain of HCV (SB strain; see Fig. S2 in the supplemental material), even though HCV replication in the lymphocytes has not been fully verified. These observations altogether demonstrate that HCV infection induces chromosomal polyploidy either in patients or in culture, as well as in blood cells or in hepatocytes.

Core protein induces chromosomal polyploidy. We next attempted to find out which viral protein is responsible for the occurrence of polyploidy. We studied the core protein, since the expression of core protein alone has been shown to induce tumors in transgenic mice (36). For this purpose, we used both a human liver cell line, HepG2, and an embryonic kidney cell line, HEK293, which stably expresses the core protein (Hep-core and 293-core), as well as a control cell line with a neomycin resistance gene (Hep-neo and 293-neo). Ploidy was charted periodically during a 6-month period. Cells were split (1:5) every 4 days. Approximately 2% of 293-neo cells showed chromosomal polyploidy initially (Fig. 2B); this frequency remained unchanged during serial passages (Fig. 2C). In contrast, the frequencies of polyploidy in the core protein-expressing cells increased as cell passage number increased (Fig. 2A and D). More than 20% of the core protein-expressing cells showed numerical chromosomal abnormalities, including polyploidy and hypertriploidy, at passage 36 (Fig. 2D). To exclude apoptosis as the cause of polyploidy and chromosomal abnormalities, apoptotic cells (annexin V^+) were gated out (Fig. 2E and F), and the nonapoptotic cells (annexin V^-) were then analyzed for the presence of polyploidy. The results showed that nonapoptotic 293-core cells displayed extensive polyploidy (Fig. 2G). Similar observations were made in HepG2 cells expressing the core protein (Fig. 2H and I). These results indicate that the core protein, by itself, can induce chromosomal polyploidy.

To exclude the possibility that chromosomal aberration was an artifact associated with cancer cell lines, we karyotyped metaphases of primary splenocytes, hepatocytes, and MEFs from 50-week-old core protein-expressing transgenic mice. The core protein-expressing transgenic mice used in this study developed tumors which originated from hepatocytes and lymphocytes at the age of 14 months and more frequent tumor development at the age of 20 months in livers and spleens (unpublished observation). Cytogenetic studies revealed that primary splenocytes of core protein-expressing transgenic mice displayed a nearly twofold higher frequency of polyploidy than that of the control mice (Fig. 3A to D). Similar results were obtained for the primary hepatocytes (Fig. 3E to I) and MEFs (see Fig. S3A in the supplemental material), although the primary hepatocytes have a high background of polyploidy even in the wild-type mice (Fig. 3I). These results indicate that HCV core protein induces polyploidy in several types of primary cells from HCV core protein-expressing transgenic mice, excluding artifactual polyploidy, which is common in cancer cell lines.

Core protein inhibits Rb and activates E2F-1 and Mad2, leading to uncoupling of the mitotic checkpoint. Polyploidy signifies defects in mitotic checkpoints. To determine the mechanism of HCV-induced defects in the mitotic checkpoint, we determined the status of Rb pathway in core-expressing cells since Rb is an upstream key regulator of these pathways (14) and core protein has been reported to downregulate Rb expression (13, 14). Core protein-expressing cells showed a reduced Rb protein level in two different hepatocyte cell lines expressing the HCV core protein (Fig. 4A). E2F-1, which is a master transcription regulator under the control of Rb (14), was correspondingly increased. Mad2, which is under the transcriptional regulation of E2F-1 and is a component of the mitotic checkpoint complex (14), was also upregulated in core-expressing cells. In contrast, Mad1 expression, which is independently regulated (6), was not affected (Fig. 4A). To determine whether alteration of Rb, Mad2, and E2F-1 expression by core protein is at the transcriptional level, these mRNAs were quantified by real-time RT-PCR. The results showed that *Rb* mRNA was significantly reduced in cells expressing the core protein (Fig. 4B), while the *e2f-1* and *mad2* mRNAs were increased (Fig. 4C and D). These results were confirmed in Raji cells infected with the SB strain of HCV (see Fig. S5A to D in the supplemental material). These results demonstrated that the transcription of these genes was affected by HCV infection and also by core protein alone.

To further confirm the overexpression of Mad2 in core protein-expressing cells, we performed immunostaining of Mad2 in stable transformants of HepG2 and HEK293 cells. The control cells expressing neomycin phosphotransferase (Hep-neo and 293-neo) did not have staining of Mad2; in contrast, Hep-core and 293-core cells had significant staining of Mad2 in the nucleus (data not shown). FACS analysis further showed that core protein-expressing cell lines had a significantly higher number of Mad2-positive cells (Fig. 4E), indicating that core protein expression induces Mad2 protein expression. These

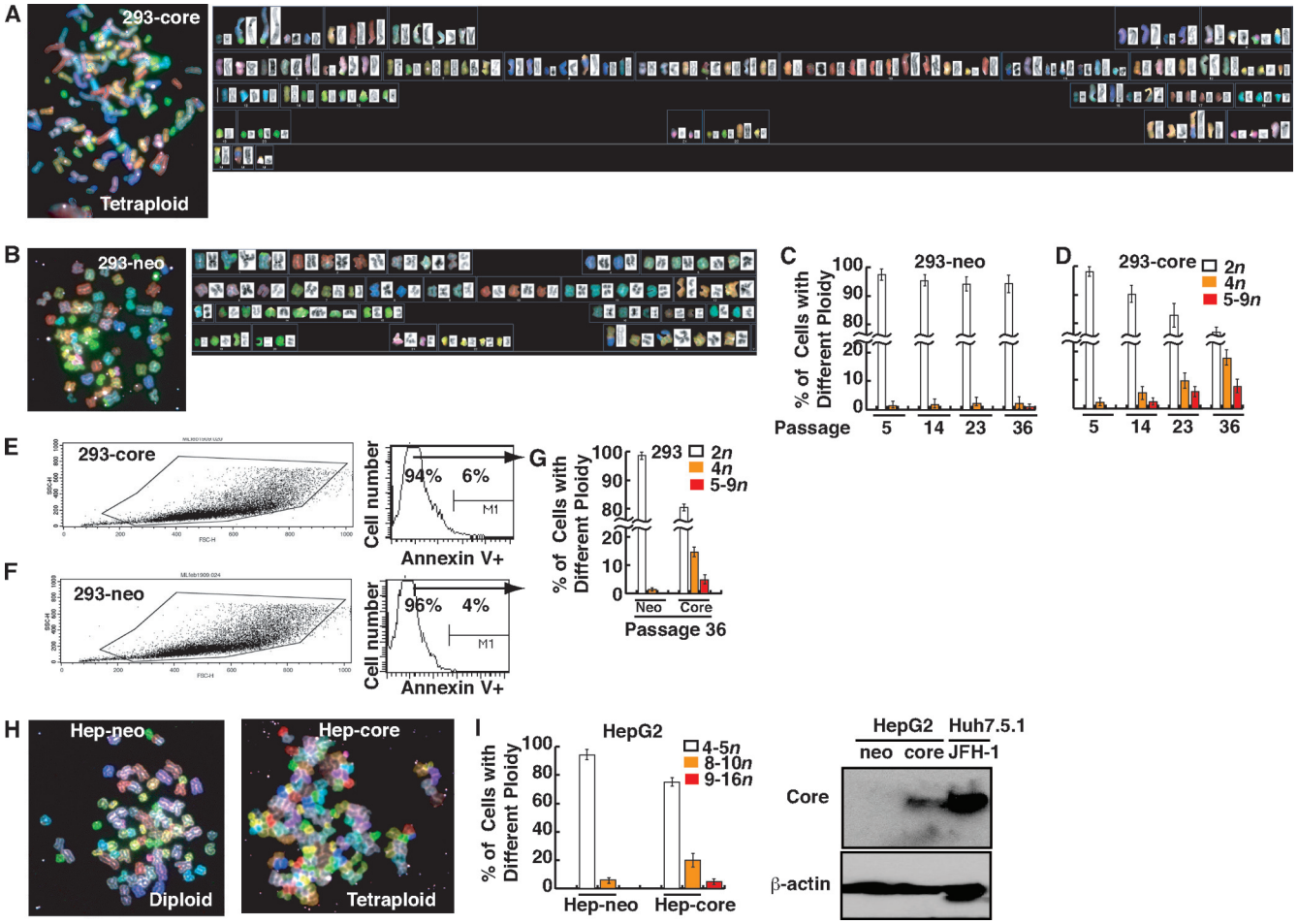

FIG. 2. Polyploidy in cell lines expressing HCV core protein. (A) Representative examples of polyploidy in HEK293 cells expressing HCV core protein (293-core). (B) Diploid chromosome from control HEK293 cells expressing the neomycin phosphotransferase (*neo*) gene (293-neo). (C and D) Percentages of cells containing polyploid chromosome numbers at different passage levels of 293-core or 293-neo cells. (E, F, and G) Percentages of cells containing polyploid chromosome numbers at passage level 36. The cells were sorted by annexin V staining. Only the nonapoptotic cells were used for karyotyping. (H) Representative examples of diploid, octaploid, and tetraploid in Hep-core and Hep-neo cells. (I) Percentages of cells containing polyploid chromosomes. The expression of core protein in HepG2 and HCV-infected Huh7.5.1 cells was confirmed by immunoblotting of core and β-actin (right insets).

data were further confirmed by luciferase reporter assay using the Rb, E2F-1, and Mad2 promoter-driven luciferase reporters in hepatocytes expressing the core protein, in which core protein inhibited the Rb promoter activity but enhanced the Mad2 promoter activity (Fig. 4F and G). The same results were obtained in lymphocytes infected with a lymphotropic strain (SB strain) of HCV (see Fig. S5E and F in the supplemental material). These results demonstrated that expression of core protein alone reduced the transcription of Rb, but activated E2F-1 and Mad2 transcription. These results are consistent with the previous reports that Rb inhibits E2F-1 and Mad2 expression (14). Furthermore, Rb promoter-driven luciferase assay performed in cells expressing individual HCV proteins showed that Rb promoter was inhibited by the core protein only, but not other viral proteins (Fig. 4H). The expression of each viral protein in this set of transfection was confirmed by RT-PCR analysis of the individual RNA (data not shown).

The inhibition of Rb transcription by the core protein has previously been reported (4); however, the mechanism of inhibition remains unclear. We therefore proceeded to characterize the promoter sequence involved in the transcriptional regulation. The analysis of truncation mutants of Rb promoter further showed that the region from nucleotide (nt) −116 to nt +186 of the Rb promoter, which includes p53-, C/EBP- and ATF/CREB-binding sites, is required for transcriptional activation (see Fig. S5G in the supplemental material). These results indicate that core protein reduces the Rb promoter activity.

To define the region of core protein involved in the inhibition of Rb promoter, a series of deletion mutants of core protein were used in the Rb promoter CAT assay. The amino acid 1-to-173 (aa 1–173), 1–153, and 1–115 deletion mutants caused reduction in Rb promoter activity to the same extent as the full-length core protein (aa 1–191) (Fig. 4I to K). However, the aa 1–81 mutant did not inhibit the Rb promoter activity ($P < 0.05$, two-sample t test) (Fig. 4K) and did not significantly induce polyploidy (Fig. 4L and M). These results demonstrate that the middle domain (aa 81–115) of core protein is critical for the inhibition of Rb promoter activity.

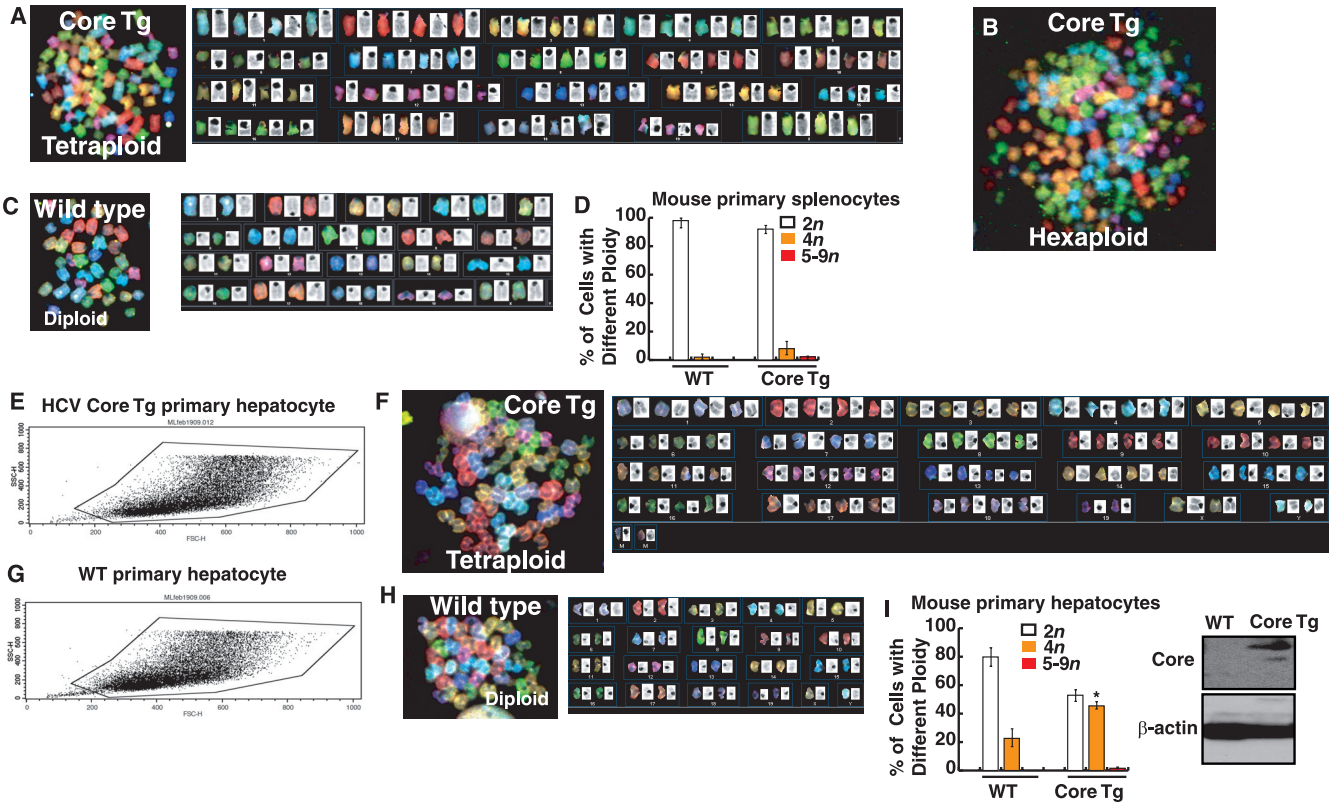

FIG. 3. Polyploidy induced by the expression of HCV core protein in mouse primary cells. (A, B, and C) Representative examples of hexaploid, tetraploid, and diploid in splenocytes from HCV core protein-expressing transgenic (Tg) or wild-type mice. (D) Percentages of polyploidy in splenocytes of core protein-expressing transgenic mice versus nontransgenic littermates. WT, wild type. (E and G) Forward and side scatter profiles of hepatocytes isolated from HCV core protein-expressing transgenic or wild-type littermates. (F and H) Representative examples of polyploidy in mouse hepatocytes from HCV core protein-expressing transgenic and wild-type mice. (I) Percentages of polyploidy in hepatocytes of core protein-expressing transgenic mice versus wild-type littermates. The expression of core protein in hepatocytes from HCV core protein-expressing transgenic mice was confirmed by immunoblotting of core and β-actin (right insets).

HCV infection or core protein impairs mitotic spindle checkpoint functions through E2F-1 overexpression. Increased frequency of polyploid metaphases from core protein-expressing cells implies possible inactivation or deregulation of mitotic spindle checkpoint function (7, 8). Furthermore, the alterations of the ratio of Mad2, Mad1, and other components of the mitotic checkpoint complex (6) in these cells suggest possible dysfunction of the mitotic checkpoint (17). We used JFH-1-infected Huh7.5.1 cells to examine this possibility. The status of HCV infection in Huh7.5.1 cells was confirmed by FACS analysis of the core protein in the infected cells (Fig. 5B). We therefore assessed the mitotic spindle checkpoint function by incubating HCV- or mock-infected Huh7.5.1 cells in colcemid for 24 h to inhibit microtubule polymerization and then quantifying DNA synthesis by BrdU incorporation. In the absence of colcemid, ~3% of HCV-infected cells (versus 1% in mock-infected cells) at day 7 were in the polyploid compartment by FACS analysis (Fig. 5A). When treated with colcemid, HCV-infected Huh7.5.1 cells at day 7 showed a more than fourfold-higher frequency of polyploidy than uninfected Huh7.5.1 cells (12% versus 3% of cells). At day 14, HCV-replicating Huh7.5.1 cells also displayed a higher frequency of polyploidy than mock-infected Huh7.5.1 cells (21% versus 3%) in the presence of colcemid treatment (Fig. 5A).

Similar results were obtained in HEK293 cell lines expressing the core protein. In the absence of colcemid, ~5% of 293-core cells (versus 2% in 293-neo cells) at passage 11 were in the polyploid compartment by FACS analysis (Fig. 5C). When treated with colcemid, 293-core cells at passage 11 showed a more than sixfold-higher frequency of polyploidy than 293-neo cells (39% versus 6% of cells). At passage 38, 293-core cells also displayed a higher frequency of polyploidy than 293-neo cells (23% versus 4%), even in the absence of colcemid treatment (Fig. 5C). These results indicate that the core protein impairs spindle checkpoint function.

To determine whether defects in the mitotic checkpoint were indeed caused by E2F-1 overexpression, we used small interfering RNA (siRNA) against *e2f-1* to downregulate E2F-1 expression (Fig. 5D). The results showed that the E2F-1 siRNA significantly reduced the expression of E2F-1 protein (Fig. 5D) and correspondingly reduced polyploidy formation (Fig. 5E), indicating that core protein-induced E2F-1 overexpression leads to the observed defects in mitotic checkpoint. To further demonstrate that the core protein-induced cascade of Rb-E2F-1-Mad2 leads to polyploidy development, we overexpressed E2F-1 or Mad2 in the HCV core cells and also used lentivirus-mediated shRNA specific for E2F-1 to downregulate E2F-1. Both E2F-1 and Mad2 overexpression caused a signif-

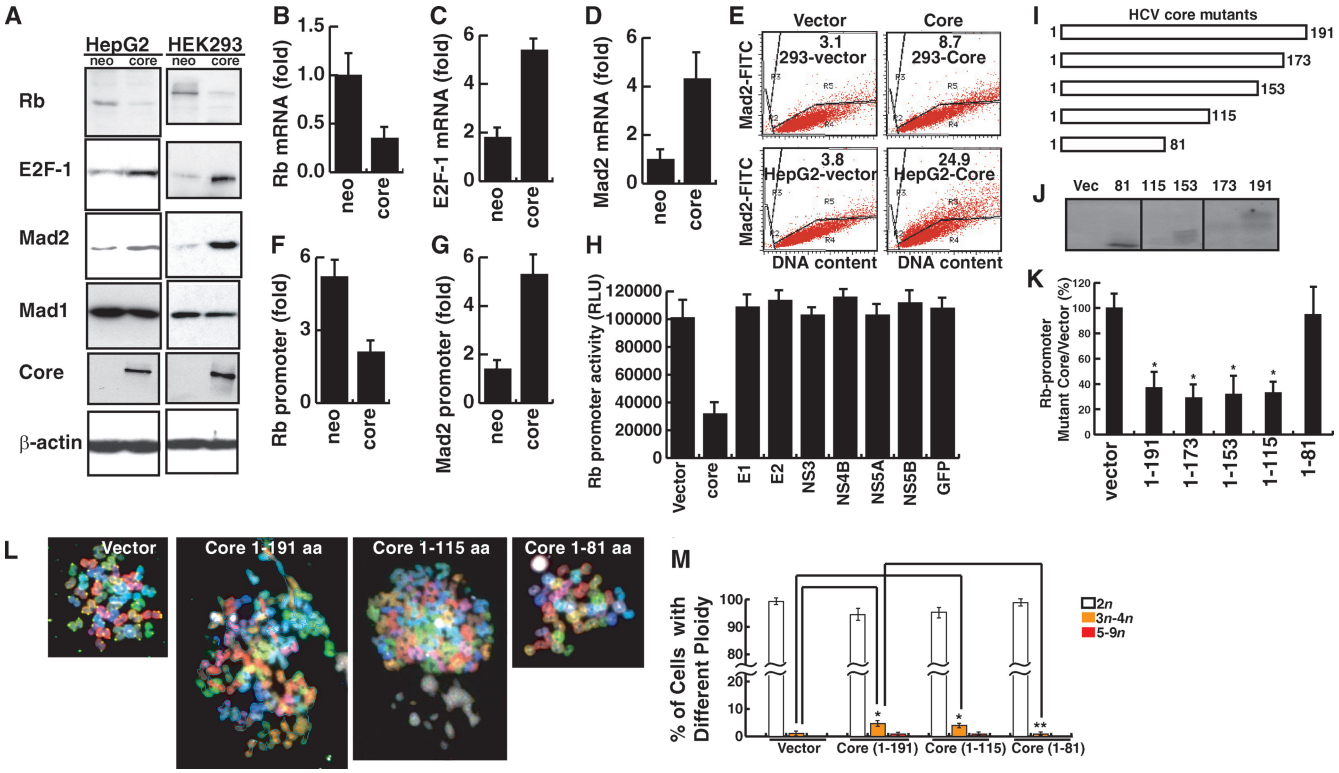

FIG. 4. Mechanism of HCV-induced mitotic spindle checkpoint defects. (A) Immunoblotting of Rb, E2F-1, and Mad2 proteins in core protein-expressing HepG2 or HEK293 cells. (B, C, and D) *Rb*, *e2f-1*, and *mad2* mRNA in core protein-stable HepG2 cells as determined by real-time RT-PCR. Relative levels of expression are indicated. (E) Flow cytometry analysis to quantify the percentage of Mad2-positive cells. Mad-2 is stained with fluorescein isothiocyanate (FITC). (F and G) Rb and Mad2-promoter-driven luciferase reporter assays in HepG2 cells expressing the core protein. (H) Rb promoter assay in HepG2 cells expressing individual viral proteins. (I) Diagram of the structure of various HCV core protein truncation mutants. (J) Translation products ([^{35}S]methionine labeling) of HCV core protein truncation variants. Vec, vector. (K) Mapping of the minimum Rb promoter sequence for the suppressive effects of HCV core protein. Huh7 cells expressing mutant core protein were transfected with an Rb promoter-CAT reporter plasmid. Forty-eight hours later, luciferase activity in the lysates was determined. Rb promoter activity was expressed as the ratio of the luciferase activity relative to that of the vector control. The data present the mean and standard deviation of five independent experiments conducted in triplicates. Asterisks indicate statistical significance ($P < 0.05$, *t* test). (L and M) Metaphase spread and percentage of cells with different polyploidy from wild-type primary splenocytes transfected with HCV core expression vectors. The full-length aa 1–191 and 1–115 truncation mutant core protein cells display preferential tetraploid, but the aa 1–81 core protein mutant and vector-transfected cells did not. Asterisks indicate statistical significance ($P < 0.05$, *t* test).

icant increase in apoptosis, as determined by annexin V or trypan blue staining (Fig. 5F and I, and see Fig. S6 in the supplemental material). Furthermore, core protein expression retarded cell growth, indicating that HCV core protein-induced dysfunction of mitotic checkpoint retarded the progression of mitosis, leading to significant increase of apoptotic cell death (Fig. 5F, H and I). Knockdown of E2F-1 in HCV core protein-expressing 293 cells restored the regular ploidy (Fig. 5E to G). These results combined indicate that overexpression of E2F-1 induces polyploidy in HCV core protein-expressing cells.

Expression of HCV core protein induces defects of mitotic segregation. To further demonstrate that E2F-1 mediates the core protein-induced mitotic segregation defects, chromosome and cytoskeleton double-staining of the core protein-expressing cells was performed. Core protein-expressing cells showed significant defects in mitotic segregation, as demonstrated by aberrant staining of tubulin and abnormal distribution of H2B (Fig. 6). This pattern was very similar to that observed in cells overexpressing E2F-1 or expressing Rb shRNA (Fig. 6) (44). When the 293-core cells were treated with E2F-1 shRNA, the H2B staining returned to normal. These results combined are consistent with the interpretation that HCV core protein expression inhibits mitotic checkpoint through E2F-1 overexpression, leading to mitotic segregation defects.

DISCUSSION

The studies presented here have demonstrated that HCV infection, or the expression of the HCV core protein alone, inhibits mitotic checkpoint functions, resulting in chromosomal polyploidy. Polyploidy was demonstrated in PBMCs of hepatitis C patients, core protein-expressing transgenic mice, and HCV-infected cell culture as well as cells expressing HCV core protein alone. Furthermore, we observed similar effects in both B cells (Raji cells and PBMCs), hepatocytes (primary hepatocytes and HepG2 and Huh7 cells), and other cell types from core protein-expressing transgenic mice (MEFs and splenocytes). Thus, these effects are likely universal. We showed that HCV infection inhibits the mitotic checkpoint

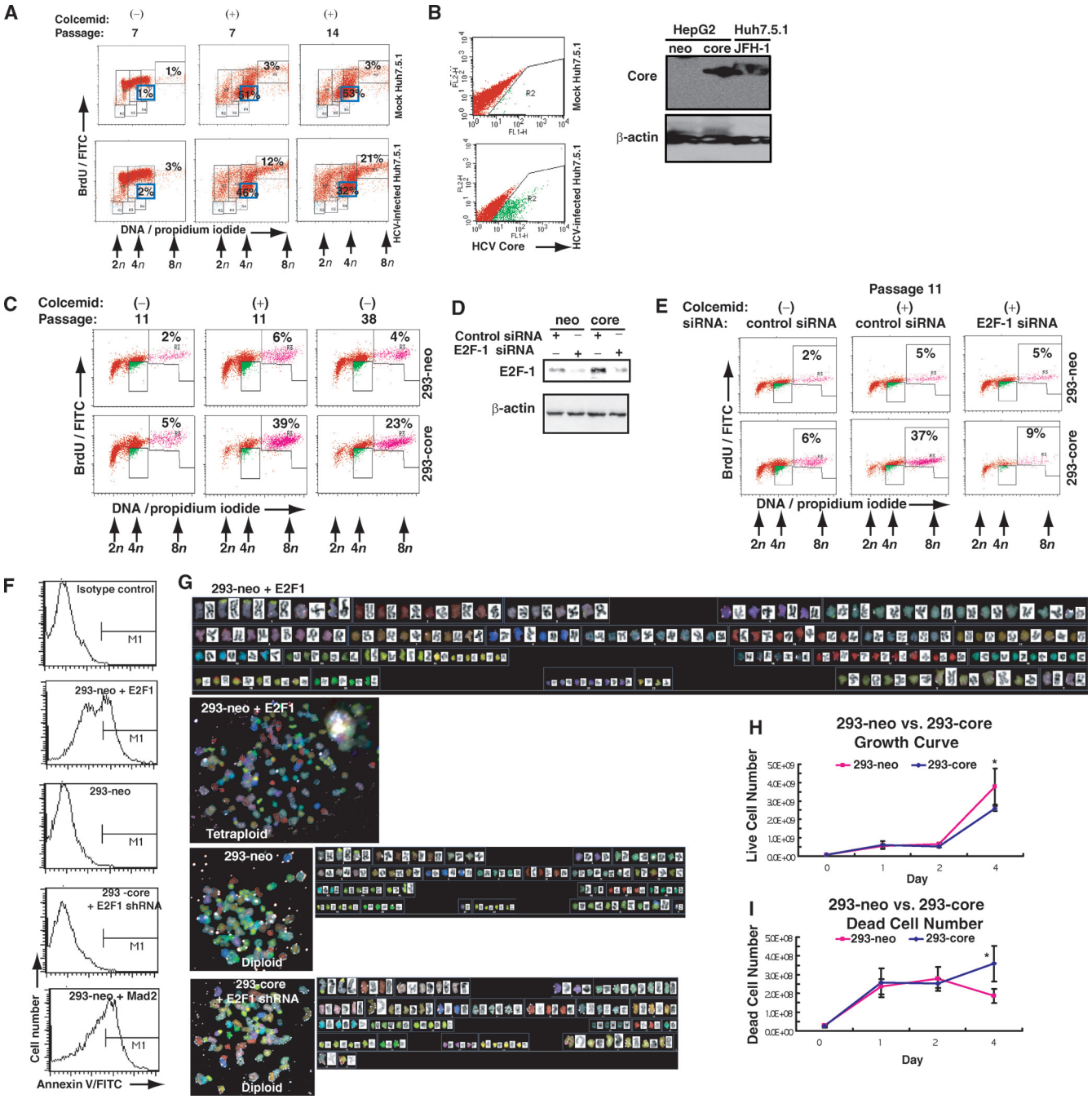

FIG. 5. Mitotic spindle checkpoint defects in HCV-infected Huh7.5.1 cells or HCV core protein-expressing HEK293 cells. (A) Mitotic spindle checkpoint function in HCV-infected Huh7.5.1 cells at different passage levels. Cells were treated with or without colcemid at two different postinfection time points, labeled with BrdU, and analyzed by FACS. The percentages of polyploid cells (>5*n*) are indicated. The boxes in the upper right quadrant represent polyploid cells. The blue square indicates the compartment of the G_2/M phase. Values are expressed as mean percentages ± standard deviations. (B) The expression of core protein in infected cells was confirmed by HCV core staining using FACS analysis and immunoblotting of core and β-actin (right insets). (C) Mitotic spindle checkpoint function in core protein-stable transformants (293-core cells) at different passage levels. Cells were treated with or without colcemid at two different passage levels, labeled with BrdU, and analyzed by FACS. The percentages of polyploid cells (>5*n*) are indicated. The boxes in the upper right quadrant represent polyploid cells. Green color indicates the compartment of the G_2/M phase. (D) Silencing of E2F-1 by siRNA in core protein-stable transformants. Cells were harvested at 4 days after siRNA transfection. Immunoblotting of E2F-1 and β-actin is shown. (E) Knockdown of E2F-1 relieves core protein-induced defects of the mitotic checkpoint. The siRNA-treated cells were stained with BrdU and propidium iodide, respectively, at 4 days posttransfection. FACS analysis was then performed. (F and G) Apoptosis in different cells was detected by staining of annexin V, followed by FACS. The nonapoptotic cells were used for karyotyping. Representative spectral karyotyping images are shown. Note that overexpression of E2F-1 shRNA restored normal diploid metaphase. FITC, fluorescein isothiocyanate. (H and I) The growth curve and dead cell number are shown for 293-neo cells (pink line) and 293-core cells (blue line).

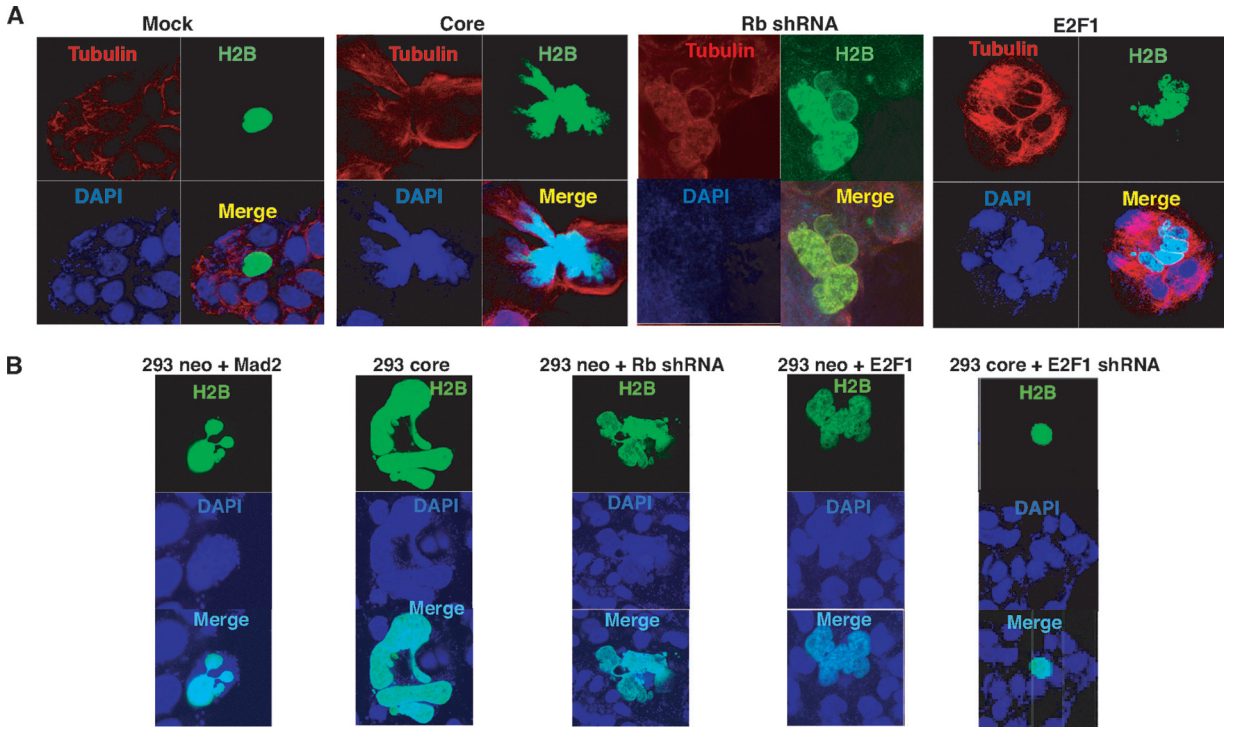

FIG. 6. Mitotic defects in HCV core protein- or E2F-1-expressing cells. (A) Mitotic segregation assay in Huh7 cells overexpressing either HCV core protein or E2F-1 or Rb shRNA. Expression vector of H2B-GFP was transfected into every set of cells. A cytoskeleton marker, β-tubulin (red), and a chromosome marker, H2B-GFP (green), were detected. Nuclei were stained by DAPI (blue). E2F-1 was overexpressed by a retrovirus vector. (B) The staining of H2B (marker for chromosomes) shows aberrant structures of nuclei in 293 cells expressing HCV core protein or Mad2, E2F-1, or Rb shRNA. The aberrant structure was restored by the E2F-1 shRNA.

through the Rb–E2F-1–Mad2 pathway (Fig. 7): namely, the core protein inhibits Rb gene transcription, leading to overexpression of E2F-1 and subsequently Mad2, the latter of which is a component of the mitotic checkpoint complex (50), which results in malfunction of the mitotic checkpoint complex. Components of mitotic checkpoints include Mad1, Mad2, Bub1, BubR1, Bub3, and the Bub3-related protein Rae1 (9). It has been shown that the ratio of these components is crucial for the formation of a functional mitotic checkpoint complex (9, 14). Complex formation is crucially regulated by ubiquitin-dependent protein degradation. The overexpression of Mad2, while Mad1 is unaffected, will disturb the normal ratio of these components in the mitotic checkpoint complex (14). The detailed mechanism of Rb suppression by core protein remains obscure (4, 13, 61). Our studies showed that the core protein inhibits Rb transcription through the suppression of the Rb promoter activity and that core protein is the only HCV protein capable of inhibiting Rb transcription. It is speculated that core protein may lift the inhibitory function of p53 on the Rb promoter (52) since core protein inhibits p53 transcription (43). We did not investigate the status of the other components of the mitotic checkpoint in this study, but the alteration of Mad2 should be sufficient to disrupt the formation of the mitotic checkpoint complex.

The effects of core proteins reported here were studied in various cell types, including primary hepatocytes and splenocytes. Thus, these findings are likely universal for all of the cell types. Interestingly, we did not observe Rb inhibition in NS5B-

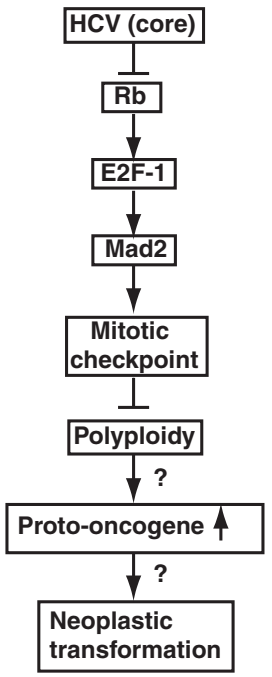

FIG. 7. Postulated mechanism of core-induced mitotic defects.

expressing cells, although it has been shown that NS5B inhibits Rb transcription (37). Differences in genotypes or cell lines may explain this discrepancy. We have ruled out cellular apoptosis as the cause of chromosome aberrations. Furthermore, these effects are not due to cell passages or associated with cancer cell lines.

In addition to polyploidy, HCV infection or core protein alone induced aneuploidy. Prototypically, a different type of spindle checkpoint defect is known to regulate aneuploidy (56). Mad2 overexpression has also been shown to promote aneuploidy, which is associated with tumorigenesis in mice, including hepatoma, lymphoma, and lung adenoma (54). However, it has been shown that Mad2 overexpression prevents aneuploidy and abnormal chromosomal segregation (15, 34); therefore, the implication of increased Mad2 expression in aneuploidy is not fully clear.

Chromosomal polyploidy is a hallmark of malignancy, including hepatocellular carcinoma (2, 22) and B-cell lymphoma (23, 39). The mechanism of polyploidy in cancer has been reported to include cleavage failure, mitotic checkpoint failure, or mitotic spindle failure (31). The downregulation of Rb gene transcription, with a resultant disruption of mitotic checkpoint complex, represents a common mechanism of viral oncogenesis. Several other viruses (human papillomavirus and simian virus 40) have been shown to cause chromosomal polyploidy by this mechanism (11, 12, 55). Epstein-Barr virus EBNA3C inhibits $p27^{KIP1}$ and abrogates the mitotic spindle checkpoint (24, 41). Furthermore, human T-cell leukemia virus Tax binds to Mad1 or the Cdc20-associated anaphase-promoting complex and activates it ahead of schedule (19, 26). By these pathways, different viruses alter mitotic checkpoint and cause cell cycle dysregulation and, consequently, polyploidy, resulting in upregulation of proto-oncogenes and downregulation of tumor suppressor genes (31, 60).

The full-length core protein is localized in the cytoplasm, but various C-terminus truncation mutants of core protein have been found in the nucleus (35, 58). These truncated forms have been shown to interact with many nuclear proteins (40). Since the mitotic checkpoint complex is localized in the nucleus, the truncation mutants of core protein are likely responsible for these effects.

Even if HCV does not replicate in B cells, but only binds to the cell surface, the signaling from the virus binding perhaps could account for these findings. We have shown that binding of HCV to the cell surface induces tumor necrosis factor alpha (28). Indeed, tumor necrosis factor alpha decreases Rb protein expression in a dose- and time-dependent manner, whereas it increases the expression level of tumor suppressor p53 protein (18).

It is not clear why human and mouse primary hepatocytes have a high background of chromosomal polyploidy. A previous study also demonstrated a similar observation in mouse primary hepatocytes (46). It could be caused by formation of undigested hepatocyte clumps or binuclear heptocytes.

In conclusion, HCV, through its core protein, causes polyploidy (Fig. 7). HCV inhibits Rb, resulting in the induction of Mad2, which is a component of the mitotic spindle checkpoint complex (51). The imbalance of the components of the mitotic checkpoint complex leads to defects in mitotic checkpoint and subsequently polyploidy. The reduced ability of HCV-infected cells to regulate the mitotic checkpoint will introduce random mutations and rearrangements into the genome, leading to predisposition to cancer. These findings open up a new avenue for investigating the mechanism of HCV-associated malignancies.

ACKNOWLEDGMENTS

We thank Chih-Lin Hsieh and Michael Lieber for advice; Claudine Kashiwabara for grammatical editing and technical assistance; Harold Soucier of the University of Southern California for FACS analysis; Takaji Wakita and Jake Liang for an expression vector of the HCV JFH-1 strain; Francis V. Chisari for Huh7.5.1 cells; and Wen-Hwa Lee at the University of California, Irvine, for Rb promoter reporter plasmids. We thank Minyi Helene Liu at USC for suggestions.

SKY was performed in the Congressman Julian Dixon Cellular Imaging Facility of the Saban Research Institute at the Los Angeles Children's Hospital. Preparation of human primary hepatocytes and immunohistochemical confocal analysis were performed in the Cell Biology Core and Cell Culture Core Facilities of the Research Center for Liver Diseases at the University of Southern California.

The study was supported by pilot project funding (5P30DK048522-13) and American Cancer Society pilot funding (IRG-58-007-48). This project was supported by Wright Foundation funding and NIH research grants 5P30DK048522-13, AI 40038, and CA108302.

REFERENCES

1. **Aoki, H., J. Hayashi, M. Moriyama, Y. Arakawa, and O. Hino.** 2000. Hepatitis C virus core protein interacts with 14-3-3 protein and activates the kinase Raf-1. J. Virol. **74:**1736–1741.
2. **Bolondi, L., L. Gramantieri, P. Chieco, C. Melchiorri, D. Trere, B. Stecca, M. Derenzini, and L. Barbara.** 1996. Enzymatic cytochemistry, DNA ploidy and AgNOR quantitation in hepatocellular nodules of uncertain malignant potential in liver cirrhosis. Dig. Dis. Sci. **41:**800–808.
3. **Chang, S. E.** 1986. In vitro transformation of human epithelial cells. Biochim. Biophys. Acta **823:**161–194.
4. **Cho, J., W. Baek, S. Yang, J. Chang, Y. C. Sung, and M. Suh.** 2001. HCV core protein modulates Rb pathway through pRb down-regulation and E2F-1 up-regulation. Biochim. Biophys. Acta **1538:**59–66.
5. **Choo, Q. L., G. Kuo, A. J. Weiner, L. R. Overby, D. W. Bradley, and M. Houghton.** 1989. Isolation of a cDNA clone derived from a blood-borne non-A, non-B viral hepatitis genome. Science **244:**359–362.
6. **Chun, A. C., and D. Y. Jin.** 2003. Transcriptional regulation of mitotic checkpoint gene MAD1 by p53. J. Biol. Chem. **278:**37439–37450.
7. **Cross, S. M., C. A. Sanchez, C. A. Morgan, M. K. Schimke, S. Ramel, R. L. Idzerda, W. H. Raskind, and B. J. Reid.** 1995. A p53-dependent mouse spindle checkpoint. Science **267:**1353–1356.
8. **Di Leonardo, A., S. H. Khan, S. P. Linke, V. Greco, G. Seidita, and G. M. Wahl.** 1997. DNA rereplication in the presence of mitotic spindle inhibitors in human and mouse fibroblasts lacking either p53 or pRb function. Cancer Res. **57:**1013–1019.
9. **Draviam, V. M., S. Xie, and P. K. Sorger.** 2004. Chromosome segregation and genomic stability. Curr. Opin. Genet. Dev. **14:**120–125.
10. **Ferri, C., F. Caracciolo, A. L. Zignego, L. La Civita, M. Monti, G. Longombardo, F. Lombardini, F. Greco, E. Capochiani, A. Mazzoni, et al.** 1994. Hepatitis C virus infection in patients with non-Hodgkin's lymphoma. Br. J. Haematol. **88:**392–394.
11. **Filatov, L., V. Golubovskaya, J. C. Hurt, L. L. Byrd, J. M. Phillips, and W. K. Kaufmann.** 1998. Chromosomal instability is correlated with telomere erosion and inactivation of G2 checkpoint function in human fibroblasts expressing human papillomavirus type 16 E6 oncoprotein. Oncogene **16:**1825–1838.
12. **Hashida, T., and S. Yasumoto.** 1991. Induction of chromosome abnormalities in mouse and human epidermal keratinocytes by the human papillomavirus type 16 E7 oncogene. J. Gen. Virol. **72:**1569–1577.
13. **Hassan, M., H. Ghozlan, and O. Abdel-Kader.** 2004. Activation of RB/E2F signaling pathway is required for the modulation of hepatitis C virus core protein-induced cell growth in liver and non-liver cells. Cell. Signal. **16:**1375–1385.
14. **Hernando, E., Z. Nahle, G. Juan, E. Diaz-Rodriguez, M. Alaminos, M. Hemann, L. Michel, V. Mittal, W. Gerald, R. Benezra, S. W. Lowe, and C. Cordon-Cardo.** 2004. Rb inactivation promotes genomic instability by uncoupling cell cycle progression from mitotic control. Nature **430:**797–802.
15. **Homer, H. A.** 2006. Mad2 and spindle assembly checkpoint function during meiosis I in mammalian oocytes. Histol. Histopathol. **21:**873–886.
16. **Honda, M., S. Kaneko, T. Shimazaki, E. Matsushita, K. Kobayashi, L. H. Ping, H. C. Zhang, and S. M. Lemon.** 2000. Hepatitis C virus core protein

induces apoptosis and impairs cell-cycle regulation in stably transformed Chinese hamster ovary cells. Hepatology **31:**1351–1359.
17. **Jeong, S. J., H. J. Shin, S. J. Kim, G. H. Ha, B. I. Cho, K. H. Baek, C. M. Kim, and C. W. Lee.** 2004. Transcriptional abnormality of the hsMAD2 mitotic checkpoint gene is a potential link to hepatocellular carcinogenesis. Cancer Res. **64:**8666–8673.
18. **Jeoung, D. I., B. Tang, and M. Sonenberg.** 1995. Effects of tumor necrosis factor-alpha on antimitogenicity and cell cycle-related proteins in MCF-7 cells. J. Biol. Chem. **270:**18367–18373.
19. **Jin, D. Y., F. Spencer, and K. T. Jeang.** 1998. Human T cell leukemia virus type 1 oncoprotein Tax targets the human mitotic checkpoint protein MAD1. Cell **93:**81–91.
20. **Jin, D. Y., H. L. Wang, Y. Zhou, A. C. Chun, K. V. Kibler, Y. D. Hou, H. Kung, and K. T. Jeang.** 2000. Hepatitis C virus core protein-induced loss of LZIP function correlates with cellular transformation. EMBO J. **19:**729–740.
21. **Kitay-Cohen, Y., A. Amiel, N. Hilzenrat, D. Buskila, Y. Ashur, M. Fejgin, E. Gaber, R. Safadi, R. Tur-Kaspa, and M. Lishner.** 2000. Bcl-2 rearrangement in patients with chronic hepatitis C associated with essential mixed cryoglobulinemia type II. Blood **96:**2910–2912.
22. **Kovi, J., E. Kovi, H. P. Morris, and M. S. Rao.** 1978. Chromosome banding patterns and breakpoints of three transplantable hepatomas induced in rats by aromatic amines. J. Natl. Cancer Inst. **61:**495–506.
23. **Kramer, A., S. Schweizer, K. Neben, C. Giesecke, J. Kalla, T. Katzenberger, A. Benner, H. K. Muller-Hermelink, A. D. Ho, and G. Ott.** 2003. Centrosome aberrations as a possible mechanism for chromosomal instability in non-Hodgkin's lymphoma. Leukemia **17:**2207–2213.
24. **Leao, M., E. Anderton, M. Wade, K. Meekings, and M. J. Allday.** 2007. Epstein-Barr virus-induced resistance to drugs that activate the mitotic spindle assembly checkpoint in Burkitt's lymphoma cells. J. Virol. **81:**248–260.
25. **Lengauer, C., K. W. Kinzler, and B. Vogelstein.** 1998. Genetic instabilities in human cancers. Nature **396:**643–649.
26. **Liu, B., S. Hong, Z. Tang, H. Yu, and C. Z. Giam.** 2005. HTLV-I Tax directly binds the Cdc20-associated anaphase-promoting complex and activates it ahead of schedule. Proc. Natl. Acad. Sci. USA **102:**63–68.
27. **Liyanage, M., A. Coleman, S. du Manoir, T. Veldman, S. McCormack, R. B. Dickson, C. Barlow, A. Wynshaw-Boris, S. Janz, J. Wienberg, M. A. Ferguson-Smith, E. Schrock, and T. Ried.** 1996. Multicolour spectral karyotyping of mouse chromosomes. Nat. Genet. **14:**312–315.
28. **Machida, K., K. T.-H. Cheng, N. Pavio, V. M.-H. Sung, and M. M.-C. Lai.** 2005. Hepatitis C virus E2-CD81 interaction induces hypermutation of the immunoglobulin gene in B cells. J. Virol. **79:**8079–8089.
29. **Machida, K., K. T.-H. Cheng, V. M.-H. Sung, K. J. Lee, A. M. Levine, and M. M. C. Lai.** 2004. Hepatitis C virus infection activates the immunologic (type II) isoform of nitric oxide synthase and thereby enhances DNA damage and mutations of cellular genes. J. Virol. **78:**8835–8843.
30. **Machida, K., K. T. Cheng, V. M. Sung, S. Shimodaira, K. L. Lindsay, A. M. Levine, M. Y. Lai, and M. M. Lai.** 2004. Hepatitis C virus induces a mutator phenotype: enhanced mutations of immunoglobulin and protooncogenes. Proc. Natl. Acad. Sci. USA **101:**4262–4267.
31. **Margolis, R. L., O. D. Lohez, and P. R. Andreassen.** 2003. G1 tetraploidy checkpoint and the suppression of tumorigenesis. J. Cell. Biochem. **88:**673–683.
32. **Martin, R. L., K. F. Ilett, and R. F. Minchin.** 1990. Characterisation of putrescine uptake by cultured adult mouse hepatocytes. Biochim. Biophys. Acta **1051:**52–59.
33. **Masuda, A., and T. Takahashi.** 2002. Chromosome instability in human lung cancers: possible underlying mechanisms and potential consequences in the pathogenesis. Oncogene **21:**6884–6897.
34. **Michel, L., R. Benezra, and E. Diaz-Rodriguez.** 2004. MAD2 dependent mitotic checkpoint defects in tumorigenesis and tumor cell death: a double edged sword. Cell Cycle **3:**990–992.
35. **Moriishi, K., T. Okabayashi, K. Nakai, K. Moriya, K. Koike, S. Murata, T. Chiba, K. Tanaka, R. Suzuki, T. Suzuki, T. Miyamura, and Y. Matsuura.** 2003. Proteasome activator PA28γ-dependent nuclear retention and degradation of hepatitis C virus core protein. J. Virol. **77:**10237–10249.
36. **Moriya, K., H. Fujie, Y. Shintani, H. Yotsuyanagi, T. Tsutsumi, K. Ishibashi, Y. Matsuura, S. Kimura, T. Miyamura, and K. Koike.** 1998. The core protein of hepatitis C virus induces hepatocellular carcinoma in transgenic mice. Nat. Med. **4:**1065–1067.
37. **Munakata, T., Y. Liang, S. Kim, D. R. McGivern, J. Huibregtse, A. Nomoto, and S. M. Lemon.** 2007. Hepatitis C virus induces E6AP-dependent degradation of the retinoblastoma protein. PLoS Pathog. **3:**1335–1347.
38. **Nahle, Z., J. Polakoff, R. V. Davuluri, M. E. McCurrach, M. D. Jacobson, M. Narita, M. Q. Zhang, Y. Lazebnik, D. Bar-Sagi, and S. W. Lowe.** 2002. Direct coupling of the cell cycle and cell death machinery by E2F. Nat. Cell Biol. **4:**859–864.
39. **Nishikori, M., H. Hansen, S. Jhanwar, J. Fried, P. Sordillo, B. Koziner, K. Lloyd, and B. Clarkson.** 1984. Establishment of a near-tetraploid B-cell lymphoma line with duplication of the 8;14 translocation. Cancer Genet. Cytogenet **12:**39–50.
40. **Owsianka, A. M., and A. H. Patel.** 1999. Hepatitis C virus core protein interacts with a human DEAD box protein DDX3. Virology **257:**330–340.
41. **Parker, G. A., R. Touitou, and M. J. Allday.** 2000. Epstein-Barr virus EBNA3C can disrupt multiple cell cycle checkpoints and induce nuclear division divorced from cytokinesis. Oncogene **19:**700–709.
42. **Ray, R. B., L. M. Lagging, K. Meyer, and R. Ray.** 1996. Hepatitis C virus core protein cooperates with *ras* and transforms primary rat embryo fibroblasts to tumorigenic phenotype. J. Virol. **70:**4438–4443.
43. **Ray, R. B., R. Steele, K. Meyer, and R. Ray.** 1997. Transcriptional repression of p53 promoter by hepatitis C virus core protein. J. Biol. Chem. **272:**10983–10986.
44. **Ren, B., H. Cam, Y. Takahashi, T. Volkert, J. Terragni, R. A. Young, and B. D. Dynlacht.** 2002. E2F integrates cell cycle progression with DNA repair, replication, and G_2/M checkpoints. Genes Dev. **16:**245–256.
45. **Ryan, C. M., E. A. Carter, R. L. Jenkins, L. M. Sterling, M. L. Yarmush, R. A. Malt, and R. G. Tompkins.** 1993. Isolation and long-term culture of human hepatocytes. Surgery **113:**48–54.
46. **Sargent, L. M., N. D. Sanderson, and S. S. Thorgeirsson.** 1996. Ploidy and karyotypic alterations associated with early events in the development of hepatocarcinogenesis in transgenic mice harboring c-myc and transforming growth factor alpha transgenes. Cancer Res. **56:**2137–2142.
47. **Sargent, L. M., G. L. Sattler, B. Roloff, Y. H. Xu, C. A. Sattler, L. Meisner, and H. C. Pitot.** 1992. Ploidy and specific karyotypic changes during promotion with phenobarbital, 2,5,2′,5′-tetrachlorobiphenyl, and/or 3,4,3′4′-tetrachlorobiphenyl in rat liver. Cancer Res. **52:**955–962.
48. **Savage, J. R.** 1976. Classification and relationships of induced chromosomal structural changes. J. Med. Genet. **13:**103–122.
49. **Schrock, E., S. du Manoir, T. Veldman, B. Schoell, J. Wienberg, M. A. Ferguson-Smith, Y. Ning, D. H. Ledbetter, I. Bar-Am, D. Soenksen, Y. Garini, and T. Ried.** 1996. Multicolor spectral karyotyping of human chromosomes. Science **273:**494–497.
50. **Shah, J. V., and D. W. Cleveland.** 2000. Waiting for anaphase: Mad2 and the spindle assembly checkpoint. Cell **103:**997–1000.
51. **Shevchenko, A., M. Wilm, O. Vorm, and M. Mann.** 1996. Mass spectrometric sequencing of proteins silver-stained polyacrylamide gels. Anal. Chem. **68:**850–858.
52. **Shiio, Y., T. Yamamoto, and N. Yamaguchi.** 1992. Negative regulation of Rb expression by the p53 gene product. Proc. Natl. Acad. Sci. USA **89:**5206–5210.
53. **Skopek, T. R., V. E. Walker, J. E. Cochrane, T. R. Craft, and N. F. Cariello.** 1992. Mutational spectrum at the Hprt locus in splenic T cells of B6C3F1 mice exposed to N-ethyl-N-nitrosourea. Proc. Natl. Acad. Sci. USA **89:**7866–7870.
54. **Sotillo, R., E. Hernando, E. Diaz-Rodriguez, J. Teruya-Feldstein, C. Cordon-Cardo, S. W. Lowe, and R. Benezra.** 2007. Mad2 overexpression promotes aneuploidy and tumorigenesis in mice. Cancer Cell **11:**9–23.
55. **Stewart, N., and S. Bacchetti.** 1991. Expression of SV40 large T antigen, but not small t antigen, is required for the induction of chromosomal aberrations in transformed human cells. Virology **180:**49–57.
56. **Storchova, Z., and D. Pellman.** 2004. From polyploidy to aneuploidy, genome instability and cancer. Nat. Rev. Mol. Cell Biol. **5:**45–54.
57. **Sung, V. M.-H., S. Shimodaira, A. L. Doughty, G. R. Picchio, H. Can, T. S.-B. Yen, K. L. Lindsay, A. M. Levine, and M. M. C. Lai.** 2003. Establishment of B-cell lymphoma cell lines persistently infected with hepatitis C virus in vivo and in vitro: the apoptotic effects of virus infection. J. Virol. **77:**2134–2146.
58. **Suzuki, R., Y. Matsuura, T. Suzuki, A. Ando, J. Chiba, S. Harada, I. Saito, and T. Miyamura.** 1995. Nuclear localization of the truncated hepatitis C virus core protein with its hydrophobic C terminus deleted. J. Gen. Virol. **76:**53–61.
59. **Takeda, S., M. Shibata, T. Morishima, A. Harada, A. Nakao, H. Takagi, and Y. Nagai.** 1992. Hepatitis C virus infection in hepatocellular carcinoma. Detection of plus-strand and minus-strand viral RNA. Cancer **70:**2255–2259.
60. **Tsuiki, H., M. Nitta, M. Tada, M. Inagaki, Y. Ushio, and H. Saya.** 2001. Mechanism of hyperploid cell formation induced by microtubule inhibiting drug in glioma cell lines. Oncogene **20:**420–429.
61. **Tsukiyama-Kohara, K., S. Tone, I. Maruyama, K. Inoue, A. Katsume, H. Nuriya, H. Ohmori, J. Ohkawa, K. Taira, Y. Hoshikawa, F. Shibasaki, M. Reth, Y. Minatogawa, and M. Kohara.** 2004. Activation of the CKI-CDK-Rb-E2F pathway in full genome hepatitis C virus-expressing cells. J. Biol. Chem. **279:**14531–14541.
62. **Tu, H., L. Gao, S. T. Shi, D. R. Taylor, T. Yang, A. K. Mircheff, Y. Wen, A. E. Gorbalenya, S. B. Hwang, and M. M. Lai.** 1999. Hepatitis C virus RNA polymerase and NS5A complex with a SNARE-like protein. Virology **263:**30–41.
63. **Vogelstein, B., and K. W. Kinzler.** 1993. The multistep nature of cancer. Trends Genet. **9:**138–141.
64. **Wakita, T., T. Pietschmann, T. Kato, T. Date, M. Miyamoto, Z. Zhao, K. Murthy, A. Habermann, H. G. Krausslich, M. Mizokami, R. Bartenschlager, and T. J. Liang.** 2005. Production of infectious hepatitis C virus in tissue culture from a cloned viral genome. Nat. Med. **11:**791–796.
65. **Xu, Y. H., G. L. Sattler, and H. C. Pitot.** 1988. A method for the comparative study of replicative DNA synthesis in GGT-positive and GGT-negative hepatocytes in primary culture isolated from carcinogen-treated rats. In Vitro Cell. Dev. Biol. **24:**995–1000.